

AUTHORS' STATEMENT: *The authors would like to thank the referees for the time and care they devoted to review this manuscript, and for their constructive comments. We have made substantial revisions to both the analysis and the presentation of the results. We hope that our responses and the significant modifications have satisfactorily addressed the concerns raised and improved the overall quality of the manuscript. Referee comments are listed below, and our responses are provided in blue font. Line numbers in our responses refer to the revised version.*

## ANONYMOUS REFEREE 1

### Summary

The paper examines the Boundary Layer over marine and West African regions. It utilizes various instruments to compute the Planetary Boundary Layer Height (PBLH) using both space-based and ground-based measurements, along with ECMWF outputs. The study discusses the similarities and differences among the various technologies and retrieval algorithms employed. It effectively characterizes the horizontal variability of the PBLH in marine and land regions during September and compare it to ECMWF retrievals. However, questions about the methodology and robustness of some analyses are problematic.

### Major comments:

- Why did you choose to use Relative Humidity (RH) to calculate the PBLH from sonde measurements, instead of using potential temperature profiles? Potential temperature is typically the more common variable utilized to derive the PBLH from radiosondes. RH measurements are often avoided due to their higher uncertainty, making them less reliable compared to potential temperature (see Liu and Liang, 2010).

We thank the reviewer for this valuable comment. We fully agree that the most scientifically robust and commonly used variables for determining the BL height from radiosondes are potential temperature and specific humidity (Seidel et al., 2010; Liu and Liang, 2010).

Relative humidity, is a variable that depends on both temperature and water vapor content, and thus varies strongly. In contrast, specific humidity is the mass of water vapor per unit mass of moist air and remains nearly conserved for an air parcel in the absence of condensation or evaporation. In our case, the radiosonde measurements were conducted on São Vicente Island in Cabo Verde, a tropical marine region characterized by a persistently humid environment. Due to this high humidity, we opted to examine the virtual potential temperature ( $\theta_V$ ), which accounts for moisture effects on air density and provides a better representation of buoyancy and atmospheric stability in moist environments.

Additionally, we observed that under such humid conditions, RH exhibits a sharp gradient at the BL top, due to the moist marine layer capped by drier air aloft. While indeed RH is not typically recommended as a primary variable for examining the BL, in our case it provided a clear empirical signal of the BL top. We present two examples of radiosonde data displaying RH, specific humidity, water vapor mixing ratio, potential temperature and virtual potential temperature in Figure 1. As we can see, the inversions (orange shading) in all the profiles for each case are located at the same level for all parameters. Therefore, this consistency supports the use of these moisture-related parameters for identifying the top of the BL. This is the reason we have included RH in Figures 3, 9, and 11 of the manuscript, where it complements the interpretation based on virtual potential temperature, but also on other measurements as well ( $V L D R_{532nm}, \beta_{1064nm}, T K E_{dr}$ ). However, our methodology section did not sufficiently explain the rationale behind the inclusion of RH in our analysis. We have revised the manuscript accordingly (lines 162-166 of the new version) to clarify this approach.

- Is there any reason why you chose to do these analyses in September? It would also be worthwhile to evaluate other months, especially when the SAL activity typically ramps up between mid-June and mid-August.

The choice of September for our analysis is primarily driven by having more homogeneous conditions

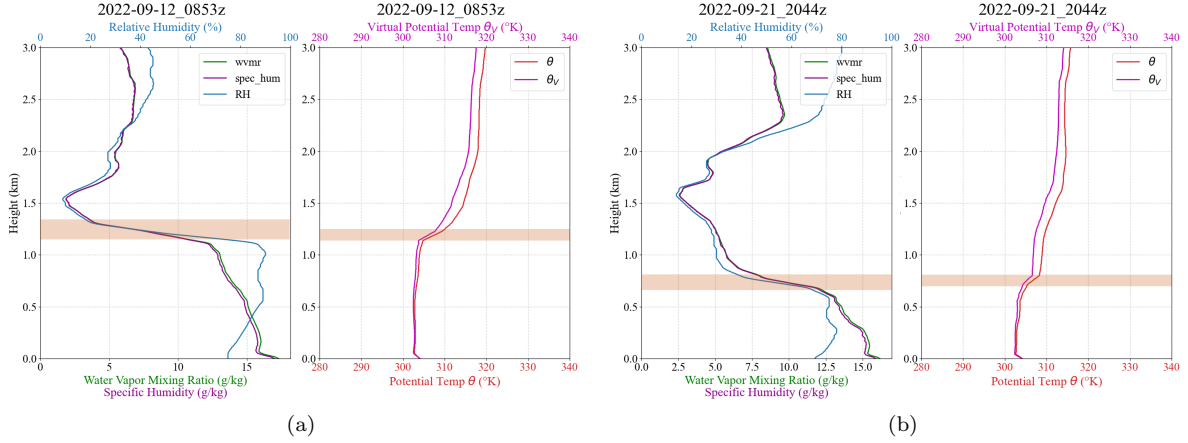


Figure 1: Moisture variables (green:water vapor mixing ratio, purple: specific humidity, blue:RH) and temperature variables (red: potential temperature ( $\theta$ ), magenta: virtual potential temperature( $\theta_v$ )) for the Radiosonde launches of (a) 12 sep 2022, 08:53 UTC and (b) 21 Sep 2022, 20:44 UTC

to better capture the prevailing environmental characteristics (lines 211-213 of the revised manuscript), but also by the data availability and the observational strategy of the ESA JATAC campaign (see this link). While the campaign extended through 2021–2022, the intensive observation phases with ground-based measurements were limited to September 2021, June 2022, and September 2022. Radiosondes were only launched during 2022, close to the ground-based lidars. These complementary datasets are critical to our study.

Furthermore, September presents distinct thermodynamic and aerosol conditions. As shown in Figure 2, sea surface temperatures are significantly warmer in September compared to June, which can influence the vertical structure of the marine boundary layer, and generally the lower troposphere dynamics. Additionally, we observed that September typically features fewer low-level clouds over the Cabo Verde region compared to June, offering clearer and more reliable lidar retrievals (Marinou et al., 2023).

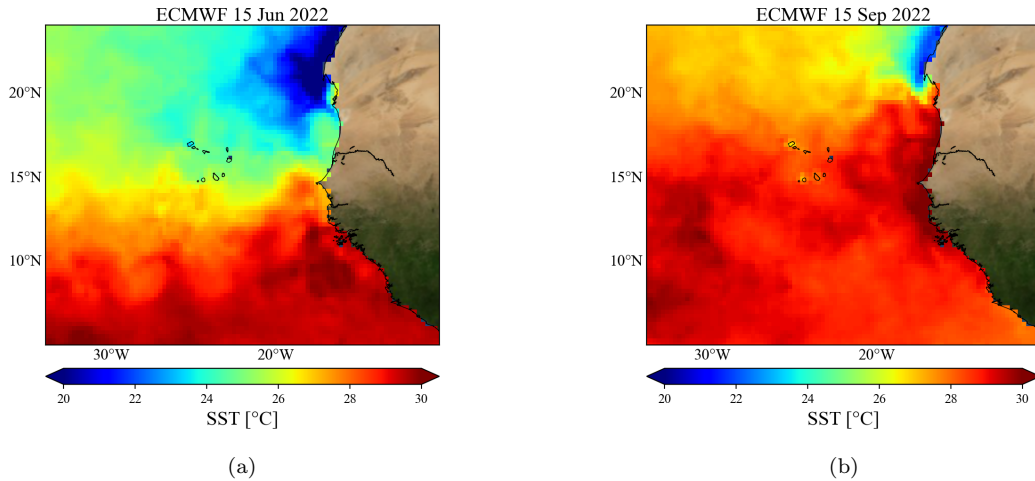


Figure 2: Sea Surface temperature (SST) from ECMWF ERA5 Reanalysis for (a) 15 June 2022 and (b) 15 Sep 2022.

Although SAL activity ramps up during mid-June to mid-August (source), dust presence remains strong through September, as we illustrate in Figure 3 for September 2021 (a) and 2022 (b). Having selected September as our focus month, we consistently compare data across the same month in different years to ensure comparable SST and seasonal conditions. Evaluating other months would be a valuable extension of this study and could be explored in future work, especially with EarthCARE now in operation.

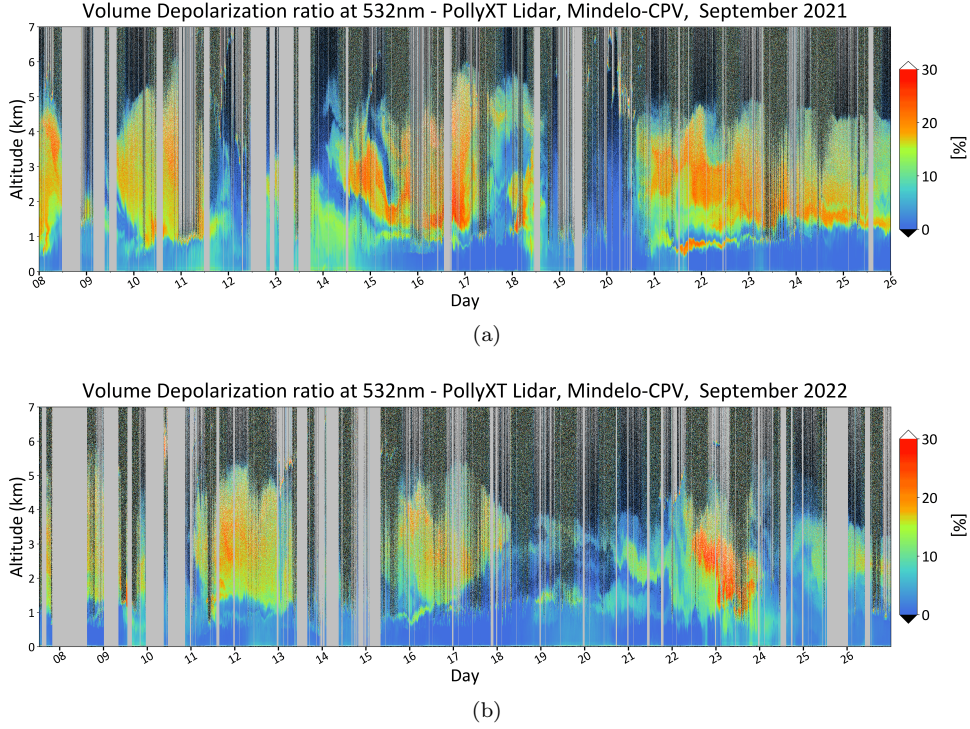


Figure 3: Volume Depolarization Ratio at 532 nm from the ground-based PollyXT Lidar in Mindelo, Cabo Verde for (a) September 2021 and (b) September 2022. The Saharan Air Layer (SAL) is present at 1-5km during almost the entire month.

- While the slope of a linear regression and the correlation coefficient are related, they are not same. The authors argue that there is a significant correlation among the different retrieved PBLHs. However, they fail to include any correlation coefficients, basing their claims solely on the slope. Additionally, the analyses presented in Sections 3.1 and 3.2 would benefit from the inclusion of scatter plots and correlation coefficients (or the  $R^2$  value from the linear regression) to better illustrate the agreement between the CALIPSO and ECMWF data. Although the mean values may be similar, the variability from day to day can differ significantly.

We thank the reviewer for pointing this out. The slope of a linear regression provides information about the scaling and potential biases between datasets, but indeed it does not capture the strength of their linear relationship. To address this, we have included the correlation coefficient ( $r$ ) in the scatter plot comparing the daily CALIPSO and ECMWF BL heights (Section 3.3, figure 7 of the new version), along with the corresponding description in the text. Furthermore, we have added an Appendix with the statistical analysis from Sections 3.1 and 3.2, that presents the distribution and intercomparison of BL heights from CALIPSO and ECMWF for Areas 1 and 2. We included normalized histograms and kernel density estimates (KDE) for both datasets, as well as scatter plots with linear regression. We modified the discussion of the following sections:

#### Section 3.1

*"The results of the MABL analysis from the space lidar data are compared with BL heights derived from the ECMWF dataset. To account for longitudinal time differences, each profile's measurement time is converted to local time based on its longitude. For each lidar profile, a temporally and spatially matched ECMWF point at the same local time is selected for direct comparison. The findings are presented in Figure 4-right. The blue circles display the MABL top heights derived from CALIPSO profiles, averaged hourly in local time. The orange points represent the corresponding hourly-averaged BL top heights from ECMWF. The data points are clustered within the 00:00–04:00 and 12:00–16:00 local time windows, because they correspond to CALIPSO's nighttime and daytime overpasses in the studied region for the month of September. The BL top in Area 1 under cloud-free conditions consistently ranges between 600 and 800 meters above sea level in both datasets. There is a strong agreement in the mean BL heights between the two datasets, each exhibiting uncertainties of approximately 20%, indicating that both provide comparable estimates of the boundary layer top. This agreement suggests that CALIPSO and ECMWF*

are consistent in representing the overall distribution of BL heights; however, as discussed in Appendix A1, their agreement at the level of individual profiles remains limited.

While uncertainties associated with BL retrievals and time averaging may broaden the range of 600-800 m for BL top, these results are consistent with the expected behavior of the MABL, which typically exhibits limited diurnal variation. The time-averaging uncertainties shown in the figure arise from the methods used to capture the BL in the two datasets. For CALIOP profiles, lidar-based retrievals inherently carry significant uncertainty and sensitivity due to measurement noise. Here, the BL top is derived using the gradient method and aerosol layers as discussed in section 2; however, this method can occasionally detect layers that do not correspond to the actual PBL, introducing additional variability. In contrast, the model provides an averaged representation over a relatively large grid ( $0.25^\circ$ , or approximately 27.8 km around  $16^\circ\text{N}$ ), which may introduce variability but is less sensitive to small-scale fluctuations compared to CALIOP. Consequently, the model typically exhibits slightly lower standard deviations.”

### Section 3.2

”In the daytime plot (Figure 6-left), the two datasets show better agreement over the ocean compared to over land. Over land, the variability increases significantly for both CALIPSO and ECMWF, sometimes reaching up to 40% (e.g., at  $\text{lon} = -8^\circ$ ), particularly for the ECMWF dataset. This increased variability can be attributed to the diurnal evolution of the boundary layer: the data include all BL tops from 06:00 to 18:00 local time. Since the boundary layer over land grows and decays throughout these hours, typical for continental and desert areas (Garcia-Carreras et al., 2015), averaging over this period naturally results in large standard deviations. A similar behavior is observed in the CALIPSO retrievals, which also show substantial variability above land. It is also worth noting that CALIPSO tends to detect lower BL tops than ECMWF over land. This difference likely arises from the way to define the BL top: ECMWF relies on thermodynamic criteria, while CALIPSO identifies a decrease in aerosol concentration. Consequently, aerosols detected by CALIPSO are mostly confined within the mixed layer (Liu et al., 2018), whereas ECMWF’s BL height may include the residual layer or even the entrainment zone above it.

In the nighttime plot (Figure 6-right), the retrieved BL tops are as expected significantly lower over land for both datasets. Over the ocean, the agreement between ECMWF and CALIPSO remains good. Over land, however, a different pattern emerges: the ECMWF dataset shows little variability but reports lower BL heights than CALIPSO, particularly further inland ( $\text{lon} > -10^\circ$ ). This again can be explained by the use of thermodynamic criteria to identify the BL top in ECMWF. In contrast, CALIPSO often detects aerosols residing in the residual layer or within the stable nocturnal boundary layer. An additional factor to consider is the quality of the CALIPSO nighttime profiles. The CALIOP instrument has different signal-to-noise characteristics during day and night: while solar background noise degrades daytime profiles, nighttime profiles suffer from lower photon count rates, which makes them noisier, especially over land (Hunt et al., 2009). This effect is consistent with our findings in Appendix A2, where the correlation between ECMWF and CALIPSO is low ( $r = 0.26$ ).

Overall, the two datasets show generally good agreement over the ocean, where both daytime and nighttime results are consistent. This aligns with the findings from section 3.1 (Area 1). The agreement is also stronger during the daytime compared to the nighttime, reflecting the limitations of the satellite nighttime measurements. Over land, however, discrepancies emerge due to the strong diurnal cycle and the different methodologies used to define the BL top.”

We hope that this additional information allows for a clearer assessment of both the agreement and variability between the two datasets.

- Constraining your analyses to only September limits your investigation’s robustness, especially in section 3.3. In the radiosonde measurements, you only have 3 cases, which does not allow you to even make any meaningful conclusion about the relationship between the retrieved PBLH from the radiosonde and CALIPSO.

We acknowledge this concern. The number of radiosondes collocated with CALIPSO overpasses at Cabo Verde is limited, since radiosondes were launched only during the 2022 intensive observation periods and not systematically aligned with CALIPSO trajectories (see line 125 of the new version). As a result, only a few cases are available for direct comparison. Nevertheless, we consider these cases valuable as they provide rare, collocated in-situ and satellite observations of the BL. While they do not allow for robust statistical conclusions, they do offer illustrative examples that support our interpretation and highlight the challenges of obtaining collocated datasets in such remote marine locations. We have revised Section 3.3 to clarify this point and to present the comparison as case-based rather than a statistical evaluation. For example we mention that ”Additionally, only three radiosonde profiles were collocated with CALIPSO overpasses during these periods, which limits the statistical robustness of the comparison. Nevertheless,



*they are included as examples of complementary in-situ measurements for the remote sensing datasets".* Moreover, we have added in the appendix A3 a correlation plot comparing the BL heights from all available radiosondes ( $N = 40$ ) with the collocated in time PollyXT Lidar retrievals to demonstrate the good agreement between the two datasets with correlation coefficient  $r = 0.87$ .

- I think the paper would benefit from a richer discussion about the improvements needed in ECMWF in representing the PBLH, especially during the continental region of West Africa, where you observed the highest differences.

We have substantially revised the sections discussing the representation of the BL height in ECMWF and the results of the comparisons, with particular attention to the continental region of West Africa where the largest differences were observed. In the revised version, we have expanded both the discussion, the methodology with more information on the ECMWF BL derivation, and the of course the conclusions. We have used all available datasets, while staying within the limits of the observational capabilities. We believe that this has allowed us to address the gaps present in the previous version as thoroughly as possible. We sincerely thank the reviewer for the valuable comments, which provided the triggering for a deeper investigation and has significantly improved the quality of the manuscript.

## Minor comments:

- Although the authors mentioned the instruments and techniques used to compute the PBLH, the description of the methodology is missing some information that will allow its reproduction. In particular, the WCT is very sensitive to the dilation factor in the Haar function, but this term is not included in the methodology section, nor are the integration limits. In addition, people typically preprocess lidar data before computing the PBLH, either by interpolating between pressure intervals or horizontally averaging to increase the SNR. I wonder if the authors made anything like this

We have revised the methodology section to ensure all details necessary for reproducing the analysis are included. In particular, we now specify the dilation factor  $\alpha$  used in the Haar WCT, which was empirically set to 100m, although it is occasionally adjusted to better capture layering. We also provide more details regarding the preprocessing of the lidar profiles: CALIPSO profiles are horizontally averaged over  $\pm 100\text{m}$  along the trajectory, while PollyXT profiles are averaged in time over  $\pm 15\text{min}$  or  $\pm 30\text{min}$ , depending on scene homogeneity. This is illustrated on the updated figure 3. Furthermore, we have reproduced the analysis using this updated CALIPSO averaging ( $\pm 100\text{m}$ ), and the results based on this approach are now included. We hope that these additions make the methodology fully transparent and reproducible, while noting that the analysis was performed for specific environments -marine or aerosol affected- and that areas with different characteristics may require tailored handling.

- L50: Spaceborne lidar signal not only attenuates as it approaches the surface due to the presence of clouds. The weakened return signals result from longer travel distances from the satellite platform to the earth's surface, which lead to a lowered SNR.

We believe the reviewer means line 150 instead of 50. We have modified the text as *"For a satellite-based lidar like CALIOP, the signal can become highly attenuated as it approaches the Earth's surface, due to the existence of clouds above the BL. The weakened return signals also result from longer travel distances from the satellite platform to the earth's surface, which lead to a lowered SNR. This can compromise the reliability of detecting lower tropospheric features and lead to inaccurate identification of the BL top. To mitigate this, i) only cloud-free profiles were selected to ensure data quality, though this restriction reduces the dataset and introduces observational limitations, and ii) averaged profiles were considered to increase the SNR"* (Lines 173-178 of the revised version).

- Figure 3: The authors mentioned that the PBLH was retrieved using both the WCT and the gradient methods for Lidar measurements. However, in Figure 3, the authors only showed the WCT for the PollyXT and the gradient for CALIPSO.

We apologize for the confusion, indeed this was not clearly presented. What we meant is that the WCT and gradient methods were applied to the ground-based and satellite lidar, respectively. We recognize that this may have been confusing, and we hope that the revised methodology section now clarifies this point.

- In line with the previous comment, you should also include in Figures 5 and 6.

the retrieved PBLH from the WCT for the CALIPSO data.

To clarify, we have applied the gradient method to the CALIPSO data, not the WCT. We apologize for any confusion and hope that this is now clear in the revised version. The WCT is a more complex method and it is a bit more difficult to apply to satellite data and less straightforward to automate. Consequently, the PBLH shown in Figures 5 and 6 is based on the gradient method, and including WCT for CALIPSO is not feasible for this study.

- Why did you choose to use Relative Humidity (RH) to calculate the PBLH from sonde measurements, instead of using potential temperature profiles? Potential temperature is typically the more common variable utilized to derive the PBLH from radiosondes. RH measurements are often avoided due to their higher uncertainty, making them less reliable compared to potential temperature (see Liu and Liang, 2010).

This point has been addressed in the response to the first major comment, where we explain that both virtual potential temperature and relative humidity were used to detect the BL top. We also note that there was an error in Figures 9 and 10, where the actual temperature was plotted; this has now been corrected.

## References

- Garcia-Carreras, L., Parker, D., Marsham, J., Rosenberg, P., Brooks, I., Lock, A., Marengo, F., McQuaid, J., and Hobby, M.: The turbulent structure and diurnal growth of the Saharan atmospheric boundary layer, *Journal of the Atmospheric Sciences*, 72, 693–713, 2015.
- Hunt, W. H., Winker, D. M., Vaughan, M. A., Powell, K. A., Lucker, P. L., and Weimer, C.: CALIPSO lidar description and performance assessment, *Journal of Atmospheric and Oceanic Technology*, 26, 1214–1228, 2009.
- Liu, B., Ma, Y., Liu, J., Gong, W., Wang, W., and Zhang, M.: Graphics algorithm for deriving atmospheric boundary layer heights from CALIPSO data, *Atmospheric Measurement Techniques*, 11, 5075–5085, 2018.
- Liu, S. and Liang, X.-Z.: Observed diurnal cycle climatology of planetary boundary layer height, *Journal of Climate*, 23, 5790–5809, 2010.
- Marinou, E., Paschou, P., Tsikoudi, I., Tsekeri, A., Daskalopoulou, V., Kouklaki, D., Siomos, N., Spanakis-Misirlis, V., Voudouri, K. A., Georgiou, T., et al.: An overview of the ASKOS campaign in Cabo Verde, *Environmental Sciences Proceedings*, 26, 200, 2023.
- Seidel, D. J., Ao, C. O., and Li, K.: Estimating climatological planetary boundary layer heights from radiosonde observations: Comparison of methods and uncertainty analysis, *Journal of Geophysical Research: Atmospheres*, 115, 2010.